

Fabrication and characterization of moderately hydrophobic membrane with enhanced permeability using a phase-inversion method in membrane distillation

Youngkwang Park^a, Jaehyun Ju^a, Yunchul Woo^b, June-Seok Choi^b, Sangho Lee^{a,*}

^a*School of Civil and Environmental Engineering, Kookmin University, Jeongneung-Dong, Seongbuk-Gu, Seoul, 136-702, Republic of Korea, Tel. +82-2-910-4529; Fax: +82-2-910-4939; emails: sanghlee@kookmin.ac.kr (S. Lee), hihiglory@gmail.com (Y. Park), jujaehyun@kookmin.ac.kr (J. Ju)*

^b*Department of Land, Water and Environment Research, Korea Institute of Civil Engineering and Building Technology, emails: yunchul84@kict.re.kr (Y. Woo), jschoi@kict.re.kr (J.-S. Choi)*

Received 30 April 2019; Accepted 9 December 2019

ABSTRACT

Although membrane distillation (MD) is considered to be a potentially useful alternative desalination process, it presents challenges including membrane fouling and potential risk of wetting. In this study, a novel approach was adopted in an attempt to address these issues. MD membranes were prepared based on the phase-inversion technique to increase their hydrophilicity (to reduce fouling) and by adjusting the polymer concentration to decrease their pore size (to reduce wetting). MD membranes were fabricated by a non-solvent induced phase separation method using solutions containing polyvinylidene fluoride (PVDF), N,N-Dimethylformamide, and LiCl. The conditions for the preparation of membranes were optimized through a series of experiments. The results showed that the optimum concentration of PVDF was 14 wt.%. Membranes prepared under the optimum conditions had a low contact angle ($75.67^\circ \pm 1.44^\circ$) and a small pore size (0.11 μm), leading to sufficient liquid entry pressure (2.93 ± 0.06 bar) for MD operation. In addition, the porosity of membranes was found to be high ($84\% \pm 0.008\%$), resulting in a higher flux (average flux 20.2 ± 0.11 L/m² h) than commercially available PVDF membrane. The membrane also showed a stable rejection ($>99.9\%$) during long-term operation.

Keywords: Fabrication membrane; Phase-inversion low hydrophobicity; High permeability; Wetting resistance

1. Introduction

Membrane distillation (MD) is a relatively novel separation process driven by thermal energy [1]. Unlike reverse osmosis (RO), the driving force behind MD is the different vapor pressure across a hydrophobic membrane. MD has a handful of advantages, including high rejection for non-volatile solutes, the capacity to treat high-salinity feed water, low electricity consumption compared with RO, and the potential to use waste heat or solar thermal energy [2–5].

These advantages mean MD is a suitable treatment option for highly concentrated industrial wastewater or zero-liquid discharge [6–8]. However, MD technology has yet to be fully commercialized because it has several drawbacks. One is the lack of appropriate membranes that have high permeability as well as low fouling and wetting properties. This has motivated a considerable number of researchers to fabricate MD membranes using various methods such as phase-inversion, electrospinning, and surface modification [9,10].

* Corresponding author.

Hydrophobicity is an important factor that affects the performance of MD membranes because it is related to resistance to pore wetting. Polymers such as polyvinylidene fluoride (PVDF) and polytetrafluoroethylene (PTFE) are relatively hydrophobic and have thus been used as materials with which to make MD membranes. Surface roughness also influences the hydrophobicity of MD membranes. Based on this factor, omniphobic MD membranes have been fabricated using an electrospinning technique [11]. Chemical modification of membrane surfaces can also change their hydrophobicity. For example, CF_4 -modified membranes have been developed and were found to be suitable for MD operations [12]. The addition of hydrophobic and hydrophilic nanoparticles to these membranes was found to be effective in increasing water flux [13]. Nevertheless, it has also been reported that an increase in the hydrophobicity of MD membranes may result in a reduction in their permeability to water.

Accordingly, for this study, we attempted a novel approach to prepare high-performance MD membranes by adjusting both their hydrophobicity and their pore size. Various membranes, with differing properties, were prepared by changing the PVDF concentration in *N,N*-dimethylformamide (DMF) solvent in a non-solvent induced phase separation (NIPS) process. The morphology of the membranes was examined using field-emission scanning electron microscopy (FE-SEM). Contact angle (CA), pore size distribution, and wetting properties were also analyzed. The permeability of the prepared MD membranes was measured in a bench-scale direct contact membrane distillation (DCMD) system and compared with that of a commercially available MD membrane. The novelty of this work lies in the fabrication of MD membranes with a moderate hydrophobicity and small pore sizes, leading to high permeability to water and low wetting tendency, which was achieved by optimizing the conditions used in the NIPS process.

2. Materials and method

2.1. Materials

PVDF (Pellets, $M_w = 530,000$ g/mol) was obtained from Sigma-Aldrich Co., USA, while DMF and LiCl were obtained from Samshun Inc., Republic of Korea. Reagent-grade sodium chloride was used to prepare the feed solution for the DCMD experiments. Deionized (DI) water was obtained using a water deionizer (HUMAN POWER, Human Co., South Korea). A casting machine (motorized film applicator, Elcometer Inc., UK) and casting knives (casting knife film applicator, Elcometer Inc., UK) were used to fabricate the membranes. Commercial PVDF membranes with a pore size of $0.22 \mu\text{m}$ (Durapore-GVHP, Millipore, USA) were purchased for comparison with the fabricated membranes.

2.2. Preparation of PVDF solution

PVDF solutions of different concentrations were prepared by dissolving PVDF pellets in DMF solvent with 3 wt.% LiCl and stirring at 200 rpm for 3 h at 80°C . The effect of additive is the catalyst that makes phase-inversion quickly. Glycerin is not a suitable additive because of its low hydrophobicity.

And the acetone used for additive was measured about low permeability. However, the addition of the LiCl in the dope solution was a strong interaction with the solvent and polymer. Also, LiCl as additive was measured about high viscosity and then made membranes improve porosity and pore size, which carried out enhancing wetting resistance [17]. The solution was then stirred at 80 rpm for 24 h before being left for 3 d at room temperature. The composition of the PVDF solutions is shown in Table 1.

2.3. Membrane fabrication

A certain concentration of PVDF solution was poured over a flat glass plate and covered by a casting knife at a thickness of $360 \mu\text{m}$. The covered film solution was immediately soaked in a coagulation bath containing DI water for 1 h. To remove any residual solvent on the surface or inside the pores, the membrane was relocated in other coagulation bath (DI water). Finally, to remove any water from the pores, the membrane was placed in an oven at 60°C for 24 h to obtain a dried, flat-sheet of the membrane.

2.4. Characterization and measurements

2.4.1. Contact angle

The CA of the membranes was measured by the sessile drop CA technique using a CA measurement device (Smart Drop, South Korea). First, membrane samples were placed on a plate and then water droplets (3–4 mL) were dropped onto the membrane surface. In a stationary state, the camera in the device captured an image of the droplet and the CA was automatically determined by the software. At least seven measurements were made for each sample and the average CA value was recorded.

2.4.2. Liquid entry pressure

Liquid entry pressure (LEP) is the minimum pressure required to enable water to penetrate a membrane's pores. LEP is affected by the hydrophobicity of the membrane, the maximum pore size, and the shape of the pores [14]. For the current study, the LEP of the membranes was measured using an in-house LEP apparatus. First, 50 mL DI water was added to the water chamber, then a dry membrane sample (with an effective surface area of 7 cm^2) was placed on the apparatus. Then nitrogen gas was supplied to the bottom of the water chamber. The pressure of the nitrogen gas was increased in a stepwise manner until the first droplet of

Table 1
Compositions of the polymer solution used for the membrane fabrication

	PVDF (wt.%)	DMF (wt.%)	LiCl (wt.%)
C-PVDF	–	–	–
PVDF 13 wt.%	13	84	3
PVDF 14 wt.%	14	83	3
PVDF 15 wt.%	15	82	3
PVDF 16 wt.%	16	81	3

water was observed on the membrane surface. To confirm reproducibility, at least three measurements were taken.

2.4.3. Membrane morphology

The samples were coated with Pt. The surfaces and cross-sections of the membranes were then examined by FE-SEM (FE-SEM 7800F Prime, JEOL Ltd. Japan).

2.4.4. Pore size and thickness

The average pore size of the membranes was estimated using a capillary flow porometer (CFP-1500-AFL, porous materials Inc.). Sample membranes were immersed in butanol and then pressed with DI water. When the pressure reached, the nitrogen gas was supplied to the samples. The flow rate under each pressure was used to calculate the pore size of the membranes. The thickness of the membranes was measured using digital Vernier calipers (Mitutoyo Inc., Japan).

2.4.5. Porosity

The membrane porosity, defined as the volume of pores divided by the total volume of the membrane, was measured using a gravimetric method [15]. Membrane samples of equal size (2 cm × 2 cm) were immersed in ethanol (Samchun Co, South Korea). The weight of the samples was measured before and after saturation with ethanol, and the membrane porosity was determined by the following equation:

$$\varepsilon = \frac{(W_1 - W_2)}{D_e} \left[\frac{(W_1 - W_2)}{D_e} + \frac{W_2}{D_p} \right] \tag{1}$$

where ε is the membrane porosity (%), W_1 is the weight of the saturated membrane (g), W_2 is the weight of the dry membrane (g), D_e is the density of the ethanol (g/cm³), and D_p is the density of the PVDF material (g/cm³).

2.4.6. X-ray diffraction

X-ray diffraction (XRD) of the membranes was measured using an instrument (TUX-3200, Smartlab, Rigaku Ltd., South Korea). In general, samples should be examined in Bragg angles ranging from 5° to 90° [16]. However, it is difficult to analyze α and β crystallites of PVDF membranes using this range of angles. Thus, the Bragg angles were limited to between 15° and 40° to increase visualization (Cu K α , $\lambda = 1.54059 \text{ \AA}$).

2.5. DCMD experiments

A series of DCMD experiments were carried out to measure the membrane’s permeability to water, based on a previously reported technique [15]. In each test, the effective membrane area was 10 cm². The flow rates for the feed water and the distillate were 0.7 and 0.4 L/min, respectively. The temperatures of the feed water and the distillate were

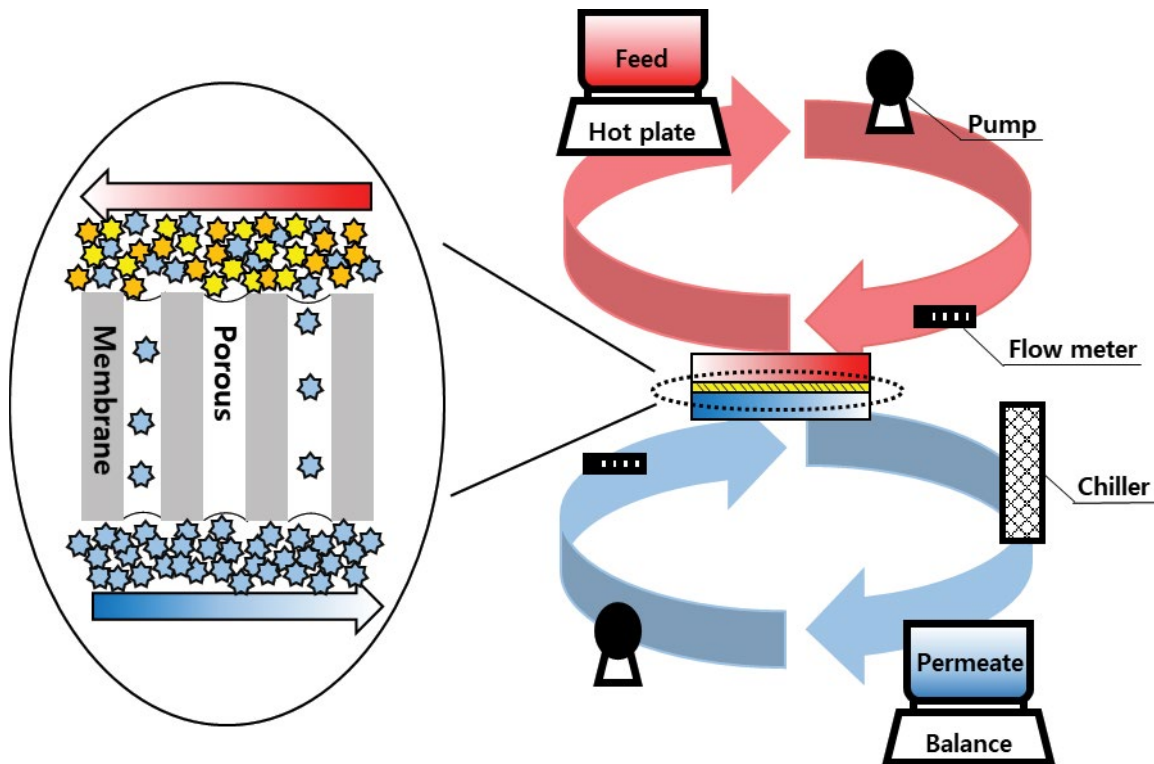


Fig. 1. Schematic diagram of the lab-scale DCMD system.

60°C ± 1.5°C and 20°C ± 1.5°C, respectively. A 35,000 mg/L NaCl solution, to simulate seawater, was used as the feed water. Conductivity was measured using a conductivity meter (WTW multi 3420, USA).

3. Results and discussion

3.1. Characterization of the fabricated membranes

The properties of the membranes fabricated under different conditions are presented and compared with those of a commercial membrane (Table 2). The commercial membrane (C-PVDF) had the highest CA, of 125.78°. As the PVDF concentration increased from 13 to 16 wt.%, the CA decreased from 79.46° ± 1.12° to 73.24° ± 2.74°. This decrease was attributed to changes in the physical properties of the membranes resulting from different PVDF concentrations, as reported in a previous study [17]. The CA of the prepared membranes is comparable with those in the literature, ranging from 57.6° ~ 90° [13,17,26]. In fact, an increase in the hydrophilicity of the membranes resulted in an increase in water flux in these works.

The porosity and pore size were also affected by the PVDF concentration. As the PVDF concentration increased from 13 wt.% to 16 wt.%, the porosity decreased from 85% ± 0.013% to 82% ± 0.023%. The mean and maximum pore sizes decreased from 0.15 to 0.07 µm and 0.142 to 0.134 µm, respectively. It should be noted that the C-PVDF membrane had a larger mean pore size (0.22 µm) and maximum pore size (2.378 µm). It seems that the fabricated membranes had smaller pores and a narrower pore-size distribution than C-PVDF.

As shown in Table 2, the LEP increased as the PVDF concentration increased. The minimum and maximum LEP values were 2.60 ± 0.22 bar and 4.16 ± 0.25 bar, respectively. The LEP is a qualitative assessment. Fabricated membranes were used in the LEP at least three-part of one membrane. And every LEP value was included in average, respectively. In this paper, other analyses were selected near the average of the fabricated membrane value. Compared with the LEP of C-PVDF (1.81 ± 0.16), they were substantially higher. This is because the LEP is a function of both hydrophobicity and pore size. Although the C-PVDF had a larger CA, it also had a larger pore size, resulting in a lower LEP compared with that of the fabricated membranes.

The thickness of the membranes increased from 95.4 ± 1.65 to 108 ± 1.85 µm with increasing PVDF concentration. Since the membranes were cast using a knife thickness of 360 µm, the solution containing a higher amount of PVDF resulted in

greater thickness. During the phase-inversion step, the solvent exchanges DI water and then polymer structures and pores formed. This phenomenon shows that the higher the ratio of solvent, the greater the decrease in membrane thickness. In general, thinner membranes may be more permeable to water due to their lower mass-transfer resistance [18]. Accordingly, it is recommended that the PVDF concentration is adjusted not only to increase the LEP but also to increase flux. This makes it difficult to determine the optimum PVDF concentration.

3.2. Morphology and structure of the fabricated membranes

Scanning electron microscopy (SEM) images of the commercial and fabricated membranes are shown in Fig. 2. The C-PVDF membrane appears to have a symmetric structure. On the other hand, the fabricated membranes show asymmetric structures, with finger-like structures in their top region and sponge-like structures in their bottom region. Although both the commercial and the fabricated membranes were made of PVDF, the morphology and structure were quite different, indicating the importance of the method used for membrane preparation.

It is evident from the SEM images that PVDF concentration affected the pore size and cross-sectional structure of the fabricated membranes. The pore size of the fabricated membranes decreased as the PVDF concentration increased (Figs. 2b–e), which matches the results shown in Table 2. The cross-sectional structure of the membranes was also affected by the PVDF concentration. When the PVDF concentration ranged from 13 to 15 wt.% (Figs. 2b–d), the bottom region of the membrane showed elongated finger-like structures. However, at a PVDF concentration of 16 wt.% (Fig. 2e), the structure of the bottom region of the membrane was sponge-like. These differences in results can be attributed to the different coagulation times resulting from different PVDF concentrations. During the NIPS process, non-solvent (DI water) diffused membrane from the top layer in the coagulation bath. If the polymer concentration is low, the diffusion of the non-solvent is fast, forming large void spaces and resulting in finger-like structures. On the other hand, the phase transition is slow if the polymer concentration is high, leading to the formation of sponge-like structures containing small voids. [19].

Fig. 3a shows the results of XRD analysis for the C-PVDF, PVDF 14 wt.%, and PVDF 16 wt.% membranes. The diffractograms for the α and β crystallites of PVDF polymers are presented in Fig. 3b [20]. The C-PVDF membrane showed

Table 2
Characteristics of commercial (C-PVDF) and fabricated membranes

Samples	Contact angle (deg)	Porosity (%)	Mean pore size (µm)	Maximum pore size (µm)	LEP (bar)	Membrane thickness (µm)
C-PVDF (Commercial)	126.78 ± 1.12	79 ± 0.027	0.22	2.378	1.81 ± 0.16	120 ± 0.75
PVDF 13 wt.%	79.46 ± 3.13	85 ± 0.013	0.15	0.142	2.60 ± 0.22	95.4 ± 1.65
PVDF 14 wt.%	75.67 ± 1.44	84 ± 0.008	0.11	0.138	2.93 ± 0.06	104.17 ± 1.24
PVDF 15 wt.%	75.27 ± 1.44	83 ± 0.002	0.11	0.137	3.43 ± 0.16	106.86 ± 1.32
PVDF 16 wt.%	73.24 ± 2.74	82 ± 0.023	0.07	0.134	4.16 ± 0.25	108 ± 1.85

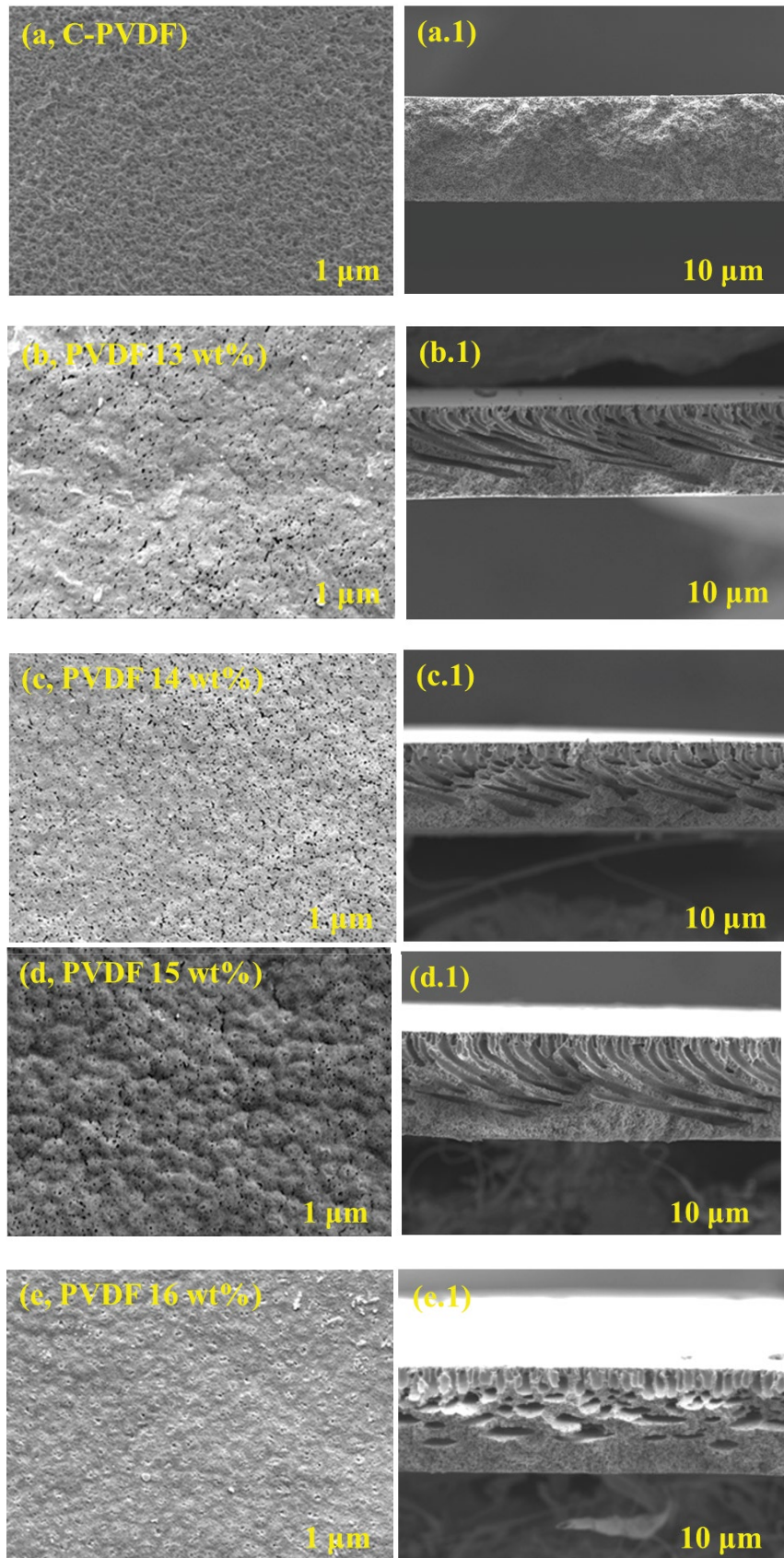


Fig. 2. Scanning electron microscopic images of the intact membranes. (a) C-PVDF membrane, (b) PVDF 13 wt.% membrane, (c) PVDF 14 wt.% membrane, (d) PVDF 15 wt.% membrane, and (e) PVDF 16 wt.% membrane.

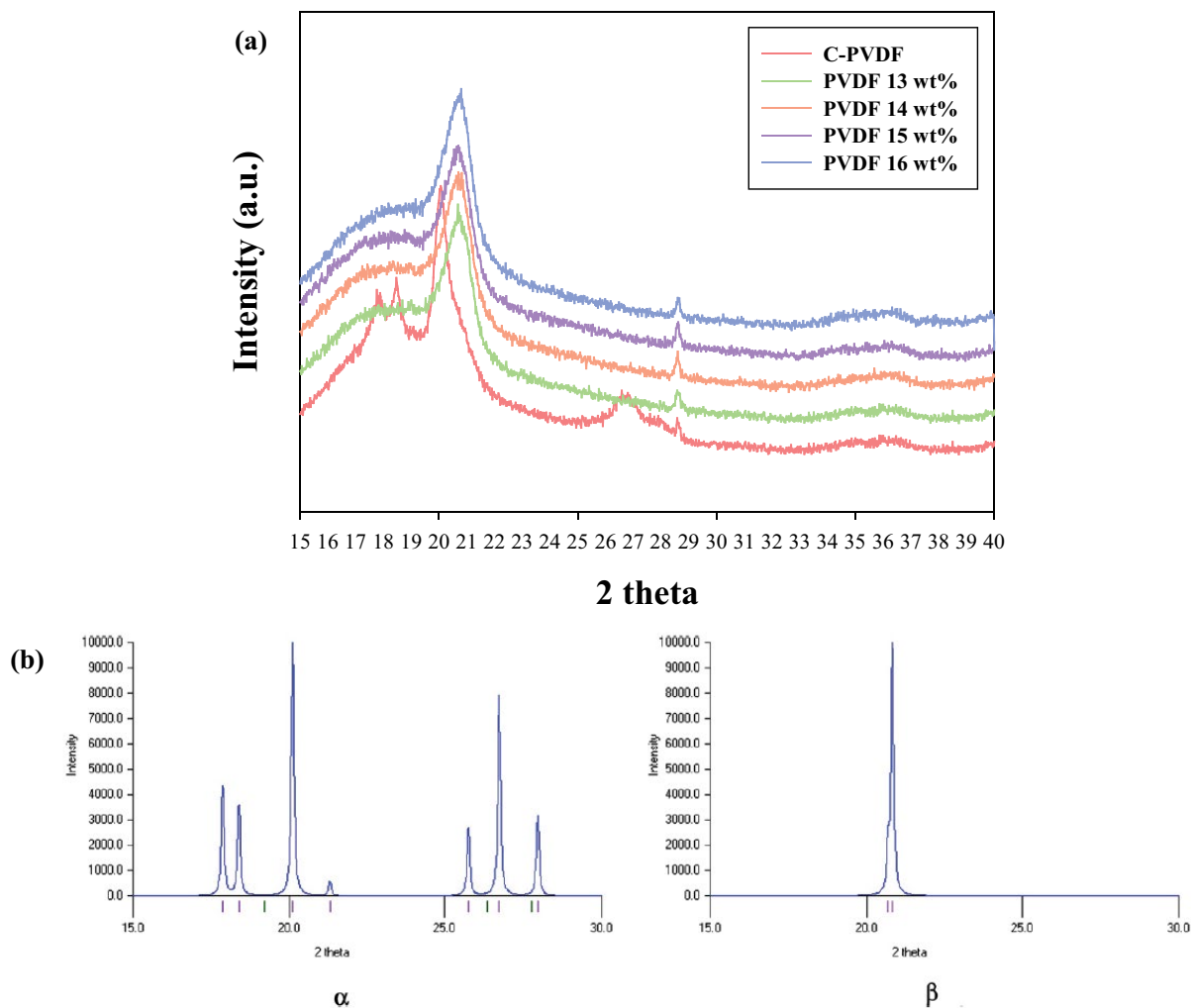


Fig. 3. (a) XRD graph of the C-PVDF, PVDF 14 wt.%, PVDF 16 wt.% membranes and (b) diffractograms of PVDF α and β crystallites in the literature [20].

peaks at 17.76° , 18.46° , 20.06° , and 26.58° , which correspond to α crystallites with planes (1 0 0), (0 2 0), (1 1 0), and (0 1 1), respectively. Among them, the peak at 20.06° was the most important, indicating that the C-PVDF membrane had the α crystallites. On the other hand, the fabricated membrane showed peaks at 20.88° , corresponding to (2, 0, 0) and (1, 1, 0). This implies that the fabricated membranes had β crystallites. The difference in the crystallinity among these membranes depends on the type of solvent and non-solvent used, and the polymer concentration. Also, the difference in crystallinity may be attributable to the difference in the temperature of the solutions during membrane fabrication. If a membrane is prepared in a solution at high temperature, it tends to form α crystallites, whereas if it is prepared in a solution at a low temperature, the membrane is likely to form β crystallites. Similar effects have been reported in the literature [21]. And fabricated membranes had β crystallites that could have enhanced flux compared with C-PVDF had α crystallites. In the reported literature, it can be seen that the PVDF membrane with crystallites (β) is measured higher flux than other membranes [25].

3.3. Flux performance of DCMD

Fig. 4 shows the water flux and distillate conductivity for the C-PVDF and the fabricated membranes in a laboratory-scale DCMD system. The feed water was a 35,000 mg/L NaCl solution. The average water flux of the C-PVDF membrane was 15.1 ± 0.61 L/m² h and the conductivity of the distillate was less than 11.8 μ S/cm (Fig. 4a). The PVDF 13 wt.% membrane showed an average flux of 14.5 ± 0.16 L/m² h and the distillate conductivity ranging from 4.1 to 83.7 μ S/cm. This wide range may be attributable to the combined effect of hydrophobicity, pore size, and porosity of this membrane. Similar results have also previously been reported [22].

The PVDF 14wt.% membrane resulted in a higher water flux (20.2 ± 0.1 L/m² h) and distillate with lower conductivity (between 4.1 and 13.6 μ S/cm) than the PVDF 13 wt.% membrane. The distillate conductivity corresponds to the NaCl rejection of over 99.975%. As PVDF concentration increased, the average flux values decreased, to 14.7 ± 0.11 L/m² h at a PVDF concentration of 15 wt.% and 8.6 ± 0.11 L/m² h

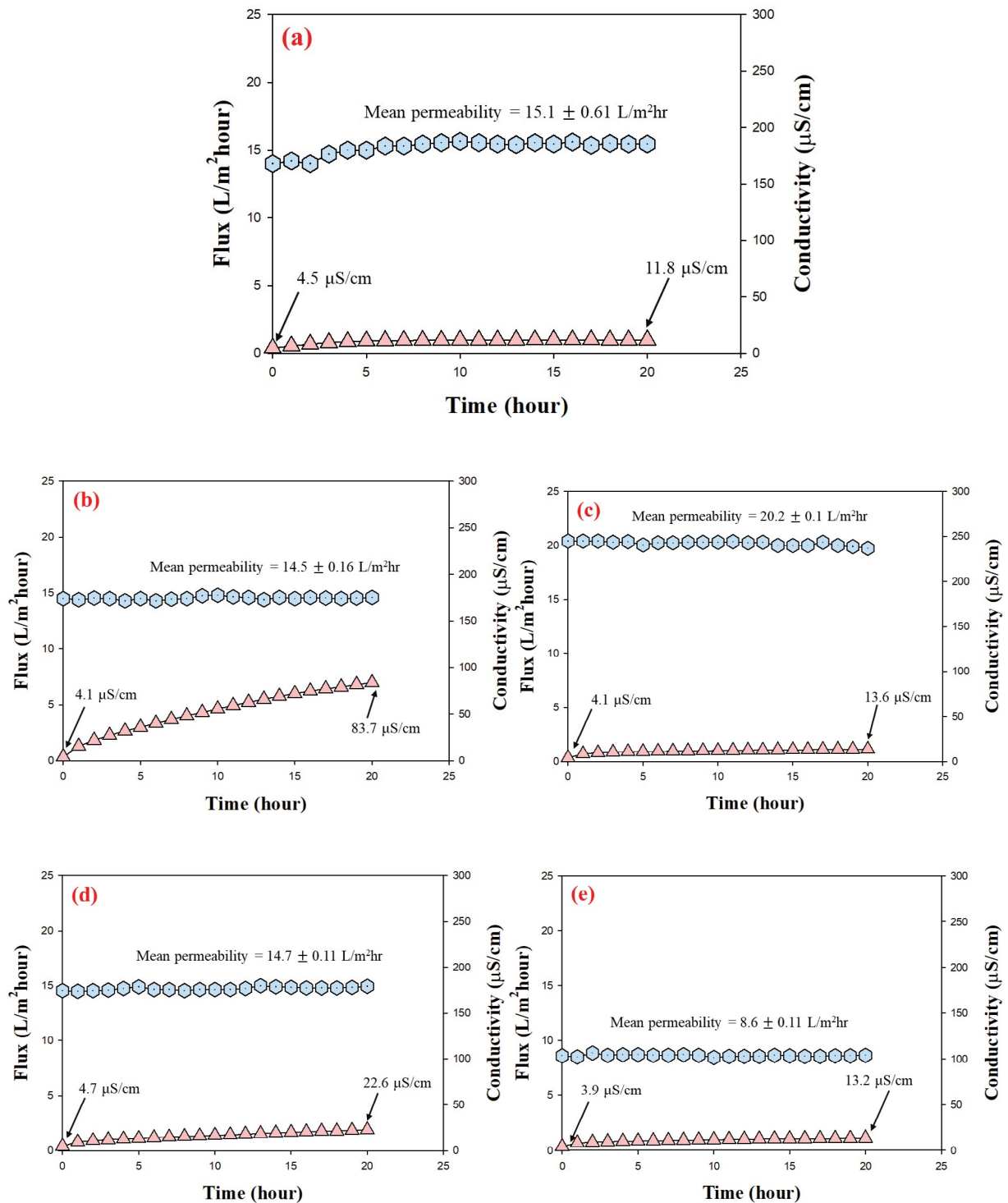


Fig. 4. Dependence of water flux and distillate conductivity on time for different membranes. (a) C-PVDF membrane, (b) PVDF 13 wt.% membrane, (c) PVDF 14 wt.% membrane, (d) PVDF 15 wt.% membrane, and (e) PVDF 16 wt.% membrane.

at a PVDF concentration of 16 wt.%. The distillate conductivities at PVDF concentrations of 15 and 16 wt.% were between 4.7 and 22.6 µS/cm and between 3.9 and 13.2 µS/cm, respectively. These results indicate that a PVDF 14 wt.% membrane is the optimum one due to its high levels of water flux and NaCl rejection.

3.4. Fouling and wetting properties

In previous experiments (Fig. 5), the water flux was measured in the absence of foulants. Here a series of experiments was carried out to compare the fouling and wetting propensities of the PVDF 14 wt.% membrane with the

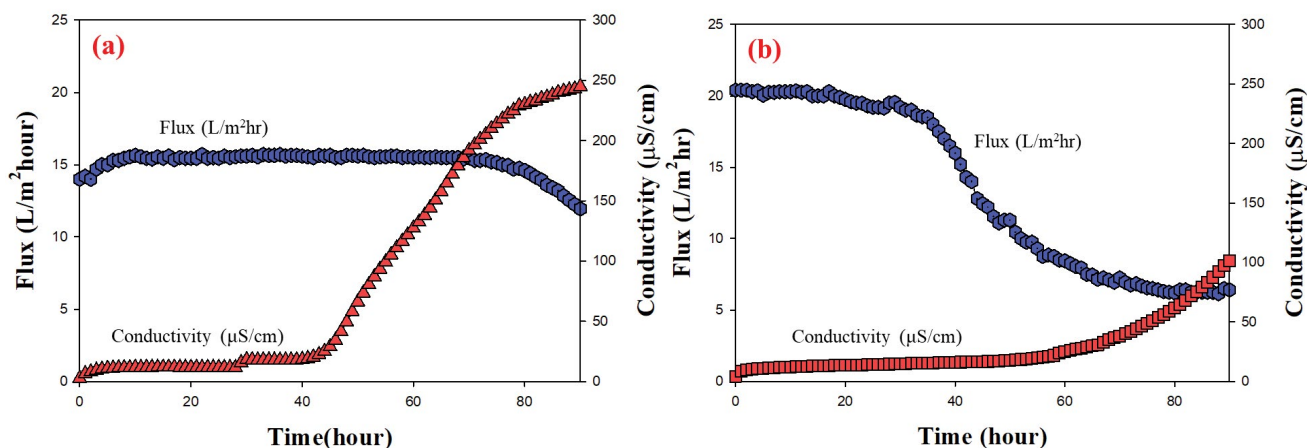


Fig. 5. Dependence of water flux and distillate conductivity on time for different membranes. (a) C-PVDF membrane and (b) PVDF 14 wt.% membrane.

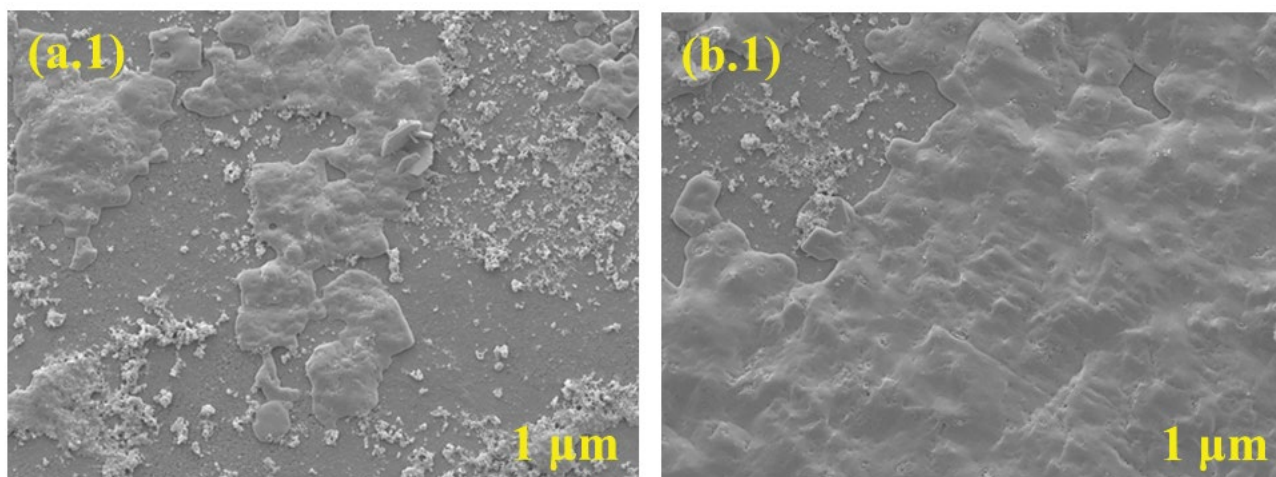


Fig. 6. Scanning electron microscopic images of the membranes fouled by NaCl scales. (a) C-PVDF membrane (b) PVDF 14 wt.% membrane.

C-PVDF membrane. The same feed solution was used but the operation time was extended to 80 h to observe fouling due to scale formation. As shown in Fig. 5a, the C-PVDF membrane showed a relatively stable flux but the distillate conductivity increased it had been in operation for approximately 40 h. This indicates that wetting occurred prior to fouling, leading to the suppression of foulant layer formation on the membrane surface. The PVDF 14 wt.% membrane exhibited flux decline after operating for 40 h, and wetting also occurred, as depicted in Fig. 5b. Nevertheless, the degree of wetting was lower for the PVDF 14 wt.% membrane than for the C-PVDF membrane. The PVDF 14 wt.% membrane had a higher resistance to wetting by fouling than the C-PVDF membrane.

Following the experiments, the membranes were analyzed using FE-SEM. As shown in Fig. 6a, the C-PVDF membrane surface was partially covered by foulant, which consisted of NaCl scales. Since this membrane was partially wetted during the experiment (Fig. 5a), its surface was not fully covered by the scales. Conversely, the PVDF 14 wt.%

membrane showed a larger amount of scale deposits than the C-PVDF membrane, which is depicted in Fig. 6b. Since the wetting was more severe for this membrane, more scales were found on its surface. Flux of PVDF 14 wt.% was measured flux decrease faster than C-PVDF in Fig. 5.

4. Conclusion

This study presents a novel approach based on the phase-inversion technique, to prepare MD membranes that have moderate hydrophobicity and small pore sizes. The following conclusions were drawn:

- The concentration of PVDF in the polymer solution significantly affects the properties of the fabricated membranes. As the PVDF concentration increased from 13 to 16 wt.%, the CA decreased from $79.46^\circ \pm 1.12^\circ$ to $73.24^\circ \pm 2.74^\circ$. The porosity and pore size decreased with increasing PVDF concentration. Both LEP and

membrane thickness increased as PVDF concentration increased.

- Although the fabricated membranes had lower hydrophobicity than the commercial (C-PVDF) membrane, they had higher permeability than the commercial membrane.
- Values due to their smaller pore sizes. This suggests that the structure of MD membranes should be optimized by adjusting both surface hydrophobicity and their pore size distribution.
- The C-PVDF membrane had a symmetric structure while the fabricated membranes showed asymmetric structures. As the PVDF concentration increased, the structure of the support changed from elongated finger-like structures to sponge-like structures.
- Considering the flux and rejection, the membrane prepared with a PVDF concentration of 14 wt.% was found to be optimum. This membrane resulted in a higher water flux (20.2 ± 0.1 L/m² h) and a distillate with lower conductivity (between 4.1 and 13.6 μ S/cm) in the DCMD experiment. The flux was approximately 25% higher than that of the C-PVDF membrane under the same operating conditions.
- The long-term DCMD experiments showed that the PVDF 14 wt.% membrane had a higher resistance to wetting by fouling than the C-PVDF membrane.

Acknowledgment

This work was supported by Korea Environment Industry & Technology Institute (KEITI) through Industrial Facilities & Infrastructure Research Program, funded by Korea Ministry of Environment (MOE) (146831).

References

- [1] K.W. Lawson, D.R. Lloyd, Membrane distillation, *J. Membr. Sci.*, 124 (1997) 1–25.
- [2] A. Razmjou, E. Arifin, G. Dong, J. Mansouri, V. Chen, Superhydrophobic modification of TiO₂ nanocomposite PVDF membranes for applications in membrane distillation, *J. Membr. Sci.*, 415 (2012) 850–863.
- [3] S. Al-Obaidani, E. Curcio, F. Macedonio, G. Di Profio, H. Al-Hinai, E. Drioli, Potential of membrane distillation in seawater desalination: thermal efficiency, sensitivity study and cost estimation, *J. Membr. Sci.*, 323 (2008) 85–98.
- [4] M. Khayet, T. Matsuura, Preparation and characterization of polyvinylidene fluoride membranes for membrane distillation, *Int. Eng. Chem. Res.*, 40 (2001) 5710–5718.
- [5] X. Yang, R. Wang, L. Shi, A.G. Fane, M. Debowski, Performance improvement of PVDF hollow fiber-based membrane distillation process, *J. Membr. Sci.*, 369 (2011) 437–447.
- [6] A.K. An, J. Guo, E.-J. Lee, S. Jeong, Y. Zhao, Z. Wang, T. Leiknes, PDMS/PVDF hybrid electrospun membrane with superhydrophobic property and drop impact dynamics for dyeing wastewater treatment using membrane distillation, *J. Membr. Sci.*, 525 (2017) 57–67.
- [7] P. Wang, T.-S. Chung, Recent advances in membrane distillation processes: Membrane development, configuration design and application exploring, *J. Membr. Sci.*, 474 (2015) 39–56.
- [8] Q. Ge, P. Wang, C. Wan, T.-S. Chung, Polyelectrolyte-promoted forward osmosis-membrane distillation (FO-MD) hybrid process for dye wastewater treatment, *Environ. Sci. Technol.*, 46 (2012) 6236–6243.
- [9] M.R. Esfahani, S.A. Aktij, Z. Dabaghian, M.D. Firouzjaei, A. Rahimpour, J. Eke, I.C. Escobar, M. Abolhassani, L.F. Greenlee, A.R. Esfahani, Nanocomposite membranes for water separation and purification: fabrication, modification, and applications, *Sep. Purif. Technol.*, 213 (2019) 465–499.
- [10] M. Khayet, Membranes and theoretical modeling of membrane distillation: a review, *Adv. Colloid Interface Sci.*, 164 (2011) 56–88.
- [11] Y.C. Woo, Y. Kim, W.-G. Shim, L.D. Tijing, M. Yao, L.D. Nghiem, J.-S. Choi, S.-H. Kim, H.K. Shon, Graphene/PVDF flat-sheet membrane for the treatment of RO brine from coal seam gas produced water by air gap membrane distillation, *J. Membr. Sci.*, 513 (2016) 74–84.
- [12] Y.C. Woo, Y. Chen, L.D. Tijing, S. Phuntsho, T. He, J.-S. Choi, S.-H. Kim, H.K. Shon, CF₄ plasma-modified omniphobic electrospun nanofiber membrane for produced water brine treatment by membrane distillation, *J. Membr. Sci.*, 529 (2017) 234–242.
- [13] Z. Li, D. Rana, Z. Wang, T. Matsuura, C.Q. Lan, Synergic effects of hydrophilic and hydrophobic nanoparticles on performance of nanocomposite distillation membranes: an experimental and numerical study, *Sep. Purif. Technol.*, 202 (2018) 45–58.
- [14] Y.C. Woo, L.D. Tijing, M.J. Park, M. Yao, J.-S. Choi, S. Lee, S.-H. Kim, K.-J. An, H.K. Shon, Electrospun dual-layer nonwoven membrane for desalination by air gap membrane distillation, *Desalination*, 403 (2017) 187–198.
- [15] L.D. Tijing, Y.C. Woo, M.A.H. Johir, J.-S. Choi, H.K. Shon, A novel dual-layer bicomponent electrospun nanofibrous membrane for desalination by direct contact membrane distillation, *Chem. Eng. J.*, 256 (2014) 155–159.
- [16] M. Buonomenna, P. Macchi, M. Davoli, E. Drioli, Poly(vinylidene fluoride) membranes by phase inversion: the role of the casting and coagulation conditions play in their morphology, crystalline structure and properties, *Eur. Polym. J.*, 43 (2007) 1557–1572.
- [17] D. Hou, H. Fan, Q. Jiang, J. Wang, X. Zhang, Preparation and characterization of PVDF flat-sheet membranes for direct contact membrane distillation, *Sep. Purif. Technol.*, 135 (2014) 211–222.
- [18] S. Nejati, C. Boo, C.O. Osuji, M. Elimelech, Engineering flat sheet microporous PVDF films for membrane distillation, *J. Membr. Sci.*, 492 (2015) 355–363.
- [19] T.-H. Young, L.-W. Chen, Pore formation mechanism of membranes from phase inversion process, *Desalination*, 103 (1995) 233–247.
- [20] R. Hasegawa, Y. Takahashi, Y. Chatani, H. Tadokoro, Crystal structures of three crystalline forms of poly (vinylidene fluoride), *Polym. J.*, 3 (1972) 600.
- [21] T.-H. Young, D.-J. Lin, J.-J. Gau, W.-Y. Chuang, L.-P. Cheng, Morphology of crystalline Nylon-610 membranes prepared by the immersion-precipitation process: competition between crystallization and liquid-liquid phase separation, *Polymer*, 40 (1999) 5011–5021.
- [22] Y.C. Woo, L.D. Tijing, W.-G. Shim, J.-S. Choi, S.-H. Kim, T. He, E. Drioli, H.K. Shon, Water desalination using graphene-enhanced electrospun nanofiber membrane via air gap membrane distillation, *J. Membr. Sci.*, 520 (2016) 99–110.
- [23] F. Meng, S.-R. Chae, A. Drews, M. Kraume, H.-S. Shin, F. Yang, Recent advances in membrane bioreactors (MBRs): membrane fouling and membrane material, *Water Res.*, 43 (2009) 1489–1512.
- [24] J. Cho, G. Amy, J. Pellegrino, Membrane filtration of natural organic matter: initial comparison of rejection and flux decline characteristics with ultrafiltration and nanofiltration membranes, *Water Res.*, 33 (1999) 2517–2526.
- [25] Z.W. Song, L.Y. Jiang, Optimization of morphology and performance of PVDF hollow fiber for direct contact membrane distillation using experimental design, *Chem. Eng. Sci.*, 101 (2013) 130–143.
- [26] M. Baghbanzadeh, D. Rana, C.Q. Lan, T. Matsuura, Effects of hydrophilic silica nanoparticles and backing material in improving the structure and performance of VMD PVDF membranes, *Sep. Purif. Technol.*, 157 (2016) 130–143.